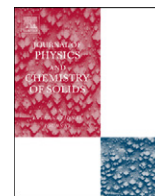




ELSEVIER

Contents lists available at ScienceDirect

## Journal of Physics and Chemistry of Solids

journal homepage: [www.elsevier.com/locate/jpcs](http://www.elsevier.com/locate/jpcs)

# Pseudogap phase of high- $T_c$ compounds described within the LDA+DMFT+ $\Sigma$ approach

I.A. Nekrasov<sup>\*</sup>, E.Z. Kuchinskii, M.V. Sadovskii

Institute for Electrophysics, Russian Academy of Sciences, Ural Branch, Ekaterinburg, Amundsen str. 106, 620016, Russia

## ARTICLE INFO

Keywords:  
D. Electronic structure

## ABSTRACT

LDA+DMFT+ $\Sigma_{\mathbf{k}}$  approach was applied to describe pseudogap phase of several prototype high- $T_c$  compounds e.g. hole doped  $\text{Bi}_2\text{Sr}_2\text{CaCu}_2\text{O}_{8-\delta}$  (Bi2212) and  $\text{La}_{2-x}\text{Sr}_x\text{CuO}_4$  (LSCO) systems and electron doped  $\text{Nd}_{2-x}\text{Ce}_x\text{CuO}_4$  (NCCO) and  $\text{Pr}_{2-x}\text{Ce}_x\text{CuO}_4$  (PCCO), demonstrating qualitative difference of the Fermi surfaces (FS) for these systems. Namely for Bi2212 and LSCO the so called “hot-spots” (intersection of a bare FS and AFM Brillouin zone (BZ) boundary), where scattering on pseudogap fluctuations is most intensive were not observed. Instead here we have Fermi arcs with smeared FS close to the BZ boundary. However, for NCCO and PCCO “hot-spots” are clearly visible. This qualitative difference is shown to have material specific origin. Good agreement with known ARPES data was demonstrated not only for FS maps but also for spectral function maps (quasiparticle bands including lifetime and interaction broadening).

© 2010 Elsevier Ltd. All rights reserved.

## 1. Introduction

One of the most prominent phenomena in high- $T_c$  cuprates physics is the so called pseudogap [1]. Here we present an overview of our recent works Refs. [2–5] on LDA+DMFT+ $\Sigma_{\mathbf{k}}$  computational scheme applications. This scheme is generalization of dynamical mean-field theory DMFT [6] and LDA+DMFT [7] (LDA—local density approximation) approach allowing to include non-local scale dependent effects [8,9]. To include pseudogap fluctuations effects important for cuprate physics we supplied (in additive manner) conventional DMFT with an external  $\mathbf{k}$ -dependent self-energy  $\Sigma_{\mathbf{k}}$ . For the pseudogap state  $\Sigma_{\mathbf{k}}$  describes the interaction of correlated electrons with non-local (quasi) static short-ranged collective Heisenberg-like AFM or SDW-like spin fluctuations [10,11].

Within LDA+DMFT+ $\Sigma_{\mathbf{k}}$  approach several high- $T_c$  prototype compounds e.g. hole doped  $\text{Bi}_2\text{Sr}_2\text{CaCu}_2\text{O}_{8-\delta}$  (Bi2212) [2] and  $\text{La}_{2-x}\text{Sr}_x\text{CuO}_4$  (LSCO) [3] as well as electron doped  $\text{Nd}_{2-x}\text{Ce}_x\text{CuO}_4$  (NCCO) [4] and  $\text{Pr}_{2-x}\text{Ce}_x\text{CuO}_4$  (PCCO) [5] were studied. Since most powerful experimental tool to access electronic properties of the pseudogap state is angular resolved photoemission spectroscopy (ARPES) [12–14] we performed comparison of LDA+DMFT+ $\Sigma_{\mathbf{k}}$  calculated spectral functions and Fermi surfaces with available ARPES quasiparticle bands and Fermi surface maps. Two-particle properties can also be described by this approach [15], e.g. calculated optical spectra in the pseudogap state compare well with experimental data for Bi2212 [2] and NCCO [4].

2. LDA+DMFT+ $\Sigma$  computational details

Crystal structure of Bi2212 [2], NCCO [4] and PCCO [5] has tetragonal symmetry with the space group  $I4/mmm$ , while LSCO has orthorhombically distorted structure  $Bmab$  [3]. For further crystallographic data used within our LDA+DMFT+ $\Sigma_{\mathbf{k}}$  approach see Refs. [2–5]. Well known quasi two-dimensional nature of these compounds determines its physical properties. Physically most interesting are the  $\text{CuO}_2$  layers. Those layers provide antibonding  $\text{Cu-}3d(x^2-y^2)$  partially filled orbital, whose dispersion crosses the Fermi level. Thus we are using this effective LDA calculated  $\text{Cu-}3d(x^2-y^2)$  antibonding band as a “bare” band in LDA+DMFT+ $\Sigma_{\mathbf{k}}$  computations. Corresponding hopping integral values obtained within the linearized muffin-tin orbitals (LMTO) method [16] and further application of the  $N$ -th order LMTO (NMTO) approach [17] are listed in Table 1.

Next to perform DMFT calculations one should set up on-site Coulomb interaction values. The values of Coulomb interaction on effective  $\text{Cu-}3d(x^2-y^2)$  orbital  $U$  obtained via constrained LDA computations [18] are also presented in the Table 1.

To account for the AFM spin fluctuations, a two-dimensional model of the pseudogap state is applied [10,11]. Corresponding  $\mathbf{k}$ -dependent self-energy  $\Sigma_{\mathbf{k}}$  [1,10,11] describes non-local correlations induced by (quasi) static short-range collective Heisenberg-like AFM spin fluctuations [19].

The  $\Sigma_{\mathbf{k}}$  definition contains two important parameters: the pseudogap energy scale (amplitude)  $\Delta$ , representing the energy scale of fluctuating SDW, and the spatial correlation length  $\xi$ . The latter is usually determined from experiment. The  $\Delta$  value was calculated as described in Refs. [8,9]. The value of correlation length was taken in accordance with the typical value obtained in neutron

\* Corresponding author.

E-mail address: [nekrasov@iep.uran.ru](mailto:nekrasov@iep.uran.ru) (I.A. Nekrasov).

scattering experiments on NCCO [21] and LSCO [22]. Employed values of  $\Delta$  and  $\xi$  for all considered systems are shown in Table 1. To solve DMFT equations numerical renormalization group (NRG, Refs. [23,24]) was employed as an “impurity solver”. Corresponding temperature of DMFT(NRG) computations was 0.011 eV and hole or electron concentrations were 15%.

### 3. Results and discussion

Based on extended analysis of LDA+DMFT+ $\Sigma_{\mathbf{k}}$  results and experimental ARPES data the origin of pronounced “hot-spots” (cross-point of the Fermi surface and umklapp surface) for electron doped systems [4,5] was established. Also it was shown that hole doped systems have only Fermi arcs [2,3]. Fig. 1 displays LDA+DMFT+ $\Sigma_{\mathbf{k}}$  spectral functions along  $1/8$  of non-interacting FS from the nodal point (top curve) to the antinodal one (bottom

**Table 1**  
Calculated energetic model parameters (eV) and experimental correlation length  $\xi$ .

	$t$	$t'$	$t''$	$t'''$	$t_{\perp}$	$U$	$\Delta$	$\xi$
Bi2212	-0.627	0.133	0.061	-0.015	0.083	1.51	0.21	10a
NCCO	-0.44	0.153	0.063	-0.01	-	1.1	0.36	50a
PCCO	-0.438	0.156	0.098	-	-	1.1	0.275	50a
LSCO	-0.476	0.077	-0.025	-0.015	-	1.1	0.21	10a

First four Cu–Cu in plain hopping integrals  $t, t', t'', t'''$ , interplain hopping value  $t_{\perp}$ , local Coulomb interaction  $U$  and pseudogap potential  $\Delta$ .

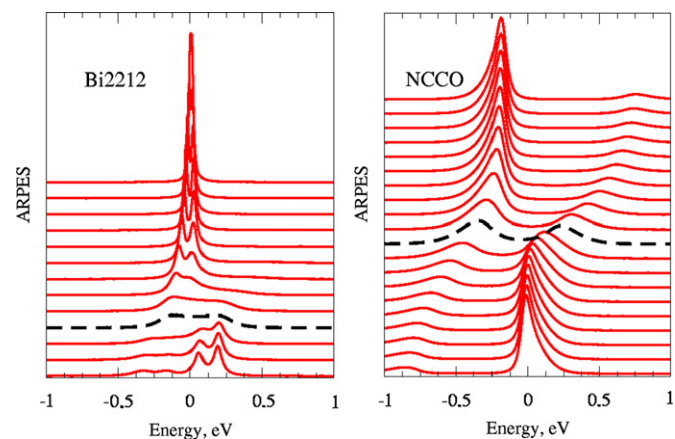


**Fig. 1.** LDA+DMFT+ $\Sigma_{\mathbf{k}}$  spectral functions for Bi2212 (upper panel) and NCCO (lower panel) along of non-interacting FS in  $1/8$  of BZ. Dashed-black line corresponds to “hot-spot” (Ref. [4]).

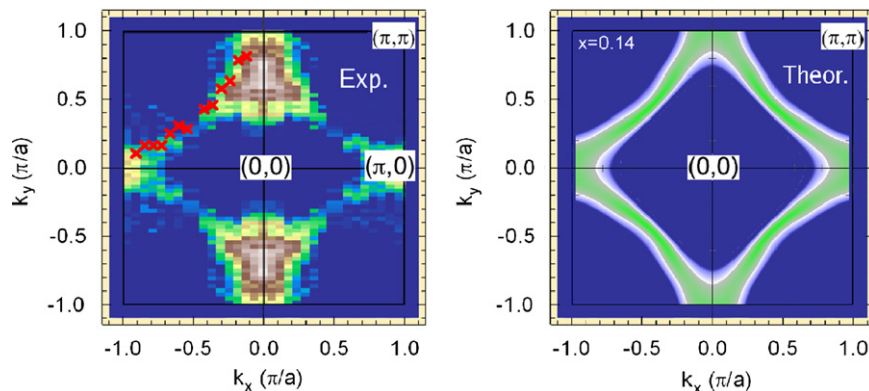


**Fig. 2.** Fermi surfaces of LSCO at  $x=0.14$  from experiment (left panel) and LDA+DMFT+ $\Sigma_{\mathbf{k}}$  computations (right panel) Red crosses on the left panel correspond to experimental  $\mathbf{k}_F$  values (Ref. [3]). (For interpretation of the references to colour in this figure legend, the reader is referred to the web version of this article.)

curve). Data for Bi2212 is given in left panel, NCCO—right panel of Fig. 1. For both compounds antinodal quasiparticles are well-defined—sharp peak close to the Fermi level. Going to the nodal point quasiparticle damping grows and peak shifts to higher binding energies. This behavior is confirmed by experiments Refs. [25,26] (for comparison with experiment see Ref. [4]). Let us interpret the spectral function peaks based on the LDA+DMFT+ $\Sigma_{\mathbf{k}}$  results. Namely, for Bi2212 nodal quasiparticles are formed by low energy edge of pseudogap, while for NCCO they are formed by higher energy pseudogap edge. Also in NCCO there is obviously no bilayer splitting effects seen for Bi2212 (left panel of Fig. 1).

“Hot-spots” for NCCO are closer to the BZ center [4]. In Fig. 1 one can see it from the position of the dashed-black line which corresponds to the “hot-spot”  $\mathbf{k}$ -point. For Bi2212 scattering from neighboring BZ amplify each other and instead of just “hot-spot” we see rather extended “deconstructed” Fermi surface towards the BZ boundaries. Such strong scattering comes from scattering processes with momentum transfer of the order of  $\mathbf{Q}=(\pi,\pi)$  [1,10,11], corresponding to AFM pseudogap fluctuations. Qualitatively the same picture is found also in LSCO (see Fig. 2).

Recent experimental and theoretical LDA+DMFT+ $\Sigma_{\mathbf{k}}$  Fermi surface maps [3] are shown in Fig. 2 at panels (a) and (b) correspondingly. Both pictures reveal strong scattering around  $(\pi,0)$ -point which we associate with scattering in the vicinity of the so-called “hot-spots” which are close to the  $(\pi,0)$  [2,4]. Along nodal directions we observe typical Fermi arcs. They are pretty well seen in the theoretical data while in experiment we observe just narrow traces of them (Bi2212 Fermi surface is compared with experiment in Ref. [2]).

Another possibility to compare LDA+DMFT+ $\Sigma_{\mathbf{k}}$  results with ARPES data is spectral function colour maps plotted along symmetry lines. In Fig. 3 we present LDA+DMFT+ $\Sigma_{\mathbf{k}}$  intensity plots along the high symmetry lines for NCCO (upper panel) in comparison with high-energy bulk sensitive angle-resolved photoemission data of  $\text{Nd}_{1.85}\text{Ce}_{0.15}\text{CuO}_4$  (lower panel) [4]. Indeed we see quite a good agreement of LDA+DMFT+ $\Sigma_{\mathbf{k}}$  and experimental data. For the  $M-\Gamma$  direction there is not very much going on. Basically we see both in theory and experiment very intensive quasiparticle band. For the  $M-\Gamma$  direction less intensive shadow band is not resolved in the experiment.

More interesting situation is observed for  $\Gamma-X-M$  directions. At  $\Gamma$ -point there is band in the experiment starting at about  $-1.2$  eV. It is rather intensive and goes up in energy. Suddenly there is almost zero intensity at about  $-0.3$  eV. Then in the vicinity of the  $X$ -point intensity rises up again. In the  $X-M$  direction around  $-0.3$  eV on the right side of  $X$ -point there is also quite intensive region. At a first glance one can think that it is the same band with

matrix element effects governing intensity. However, based on analysis of Ref. [4] one can conclude that this low intensity region is the forbidden gap between shadow and quasiparticle bands. The “horseshoe” around X-point is formed by the shadow band on the left and the quasiparticle band on the right for upper branch and other way round for the lower branch. As a consequence of that there is also intensive shadow FS sheets around  $(\pi/a, 0)$  point. Rather intensive non-dispersive states at about  $-1.0$  eV within experimental data can be presumably associated with the lower Hubbard band and possible admixture of some oxygen states. Let us also suppose that high intensity at  $-0.3$  eV for X point may be interpreted not as a van-Hove singularity of bare dispersion but rather of high-energy pseudogap branch [4].

One more fascinating comparison for LDA+DMFT+ $\Sigma_k$  results with experimental ARPES data is recently reported by us in the Ref. [5]. In Fig. 4 an extended picture of PCCO Fermi surfaces is presented (panel (a) LDA+DMFT+ $\Sigma_k$  results, panel (b) experimental ARPES data). Strictly speaking Fig. 4 is a color map in reciprocal space of the corresponding spectral function plotted at the Fermi level. FS is clearly

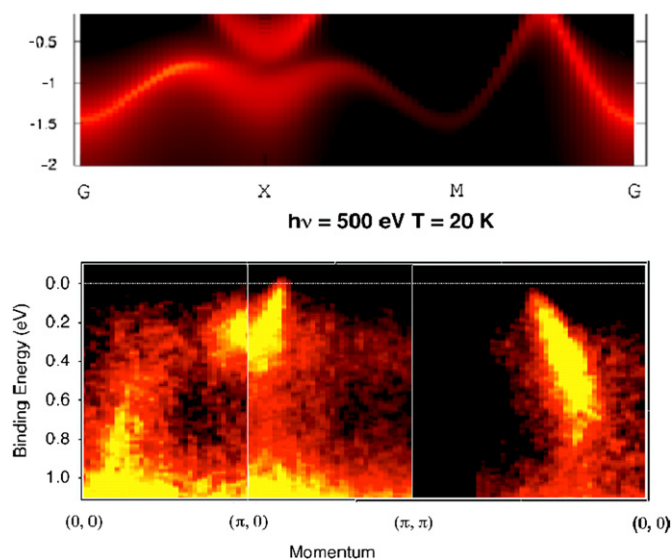


**Fig. 3.** Comparison of LDA+DMFT+ $\Sigma_k$  spectral functions (upper panel) for NCCO along BZ high-symmetry directions with experimental ARPES (Ref. [4]) (lower panel).

visible as reminiscence of non-interacting band close to the first Brillouin zone border and around  $(\pi/2, \pi/2)$  point (so called Fermi arc), where the quasiparticle band crosses the Fermi level. There is an interesting physical effect of partial “destruction” of the FS observed in the “hot-spots”, points that are located at the intersection of the FS and its AFM umklapp replica. This FS “destruction” occurs because of the strong electron scattering on the antiferromagnetic (AFM) spin (pseudogap) fluctuations on the copper atoms. Also the “shadow” FS is visible as it should be for AFM folding. As no long-range order is present in the underdoped phase the “shadow” FS has weaker intensity with respect to FS. The PCCO FS is very similar to that of  $\text{Nd}_{2-x}\text{Ce}_x\text{CuO}_4$  (NCCO), which belongs to the same family of superconductors [4,25].

Let us compare theoretical (upper panels) and experimental (lower panels) energy quasiparticle dispersion for most characteristic cuts introduced in Fig. 4 (see Fig. 5). Theoretical data were multiplied by the Fermi function at a temperature of 30 K and convoluted with a Gaussian to simulate the effects of experimental resolution, with further artificial noise added.

The Cut 1 intersects quasiparticle and “shadow” Fermi surfaces close to the Brillouin zone border. One can find here a “fork”-like structure formed by the damped “shadow” band ( $-0.5$  to  $0$  arb.u.) and better defined quasiparticle band ( $0.5$ - $1$  arb.u.). This structure corresponds to preformation of FS cylinder around  $(\pi, 0)$  point. The Cut 2 goes exactly through the “hot-spot”. Here we see a strong suppression of the quasiparticle band around the Fermi level similar to NCCO as shown in Fig. 3. The Cut 3 crosses the Fermi arc, where we can see a very well defined quasiparticle band. However, weak intensity “shadow” band is also present. For the case of long range AFM order and complete folding of electronic structure, FS and its “shadow” should form a closed FS sheet around  $(\pi/2, \pi/2)$  point, while in the current case the part of the pocket formed by the “shadow” band is not so well defined in momentum space. As can be seen there is a good correspondence between the calculated and experimental data in terms of the above described behavior, which is also similar to the results reported for  $\text{Nd}_{2-x}\text{Ce}_x\text{CuO}_4$  (NCCO) in our earlier work [4].

#### 4. Conclusion

Here we summarize our recent results on LDA+DMFT+ $\Sigma_k$  investigations of pseudogap state for a number of copper high- $T_c$  compounds. We considered for the main prototype systems: hole

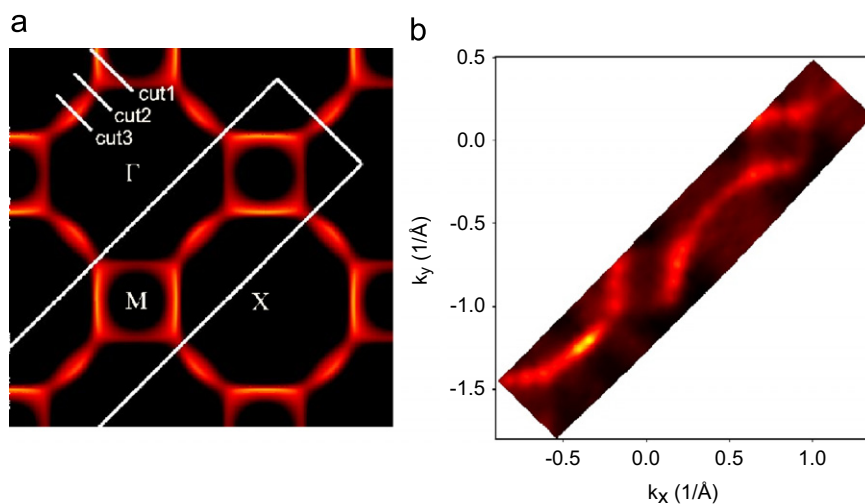


**Fig. 4.** (a) Extended Fermi surfaces for PCCO—LDA+DMFT+ $\Sigma_k$  data. White rectangle on panel (a) schematically shows the part of reciprocal space measured experimentally (panel b). Lower left corner is X-point  $(\pi, 0)$  (Ref. [5]).

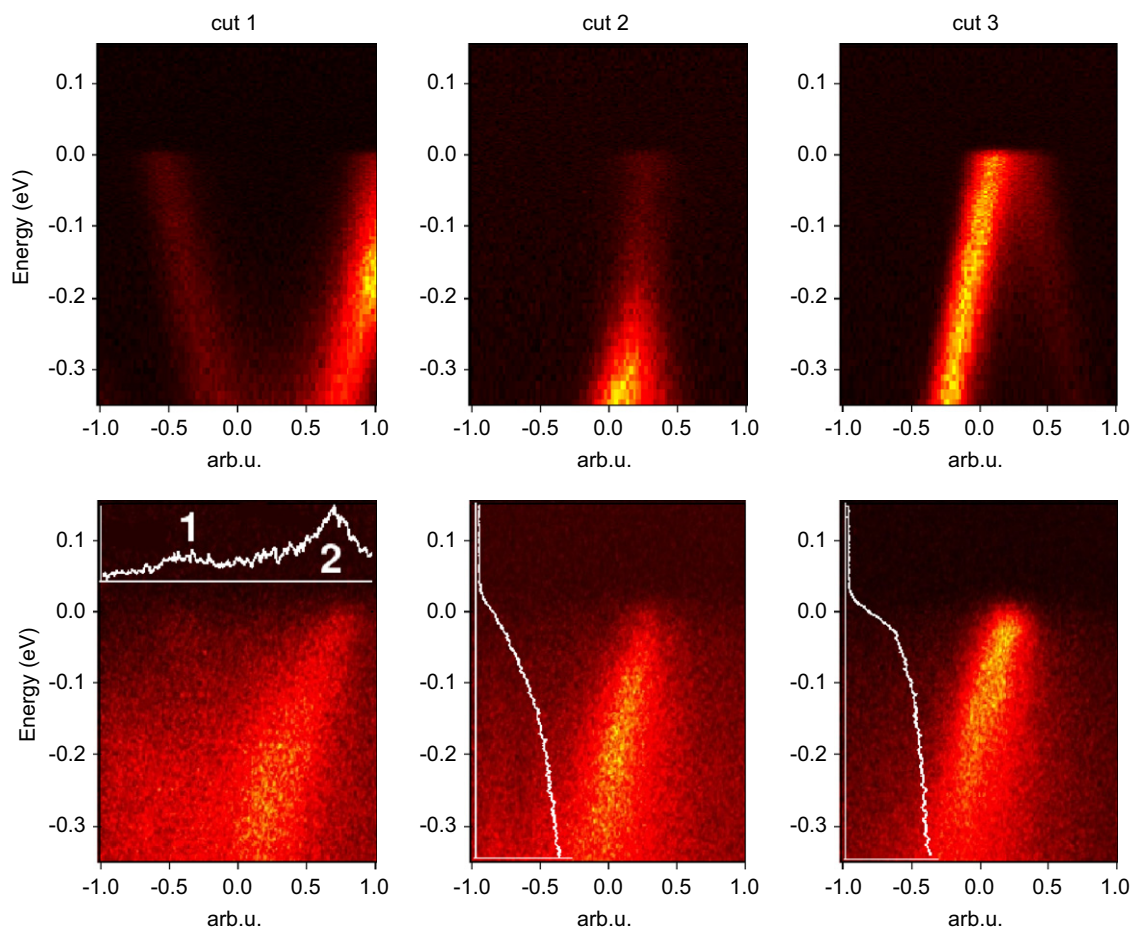


**Fig. 5.** Energy–momentum intensity distributions for the specific cuts drawn in Fig. 4 (upper panels—theoretical data, lower panels—experimental photoemission intensity). To judge about the absolute intensities of the “shadow” (1) and main band (2) cut 1 contains an MDC curve integrated in an energy window 60 meV centered at the Fermi level (FL). Similarly integral EDC for cut 2 (“hot-spot”) shows suppression of the intensity at the FL as compared to cut 3, which is located further away from the “hot-spot” (Ref. [4]). The FL is zero.

doped—Bi2212 [2] and LSCO [3]; electron doped—PCCO [5] and NCCO [4]. For all compounds the LDA+DMFT+ $\Sigma_{\mathbf{k}}$  calculations show that Fermi-liquid behavior is still conserved far away from the “hot-spots” (antinode direction), while the destruction of the Fermi surface observed in the vicinity of “hot-spots” (close to nodal direction). This destruction is due to strong scattering of correlated electrons on short-range antiferromagnetic (pseudogap) fluctuations. Moreover the origin of clearly observed “hot-spots” for electron doped systems (in contrast to hole doped ones with a Fermi arcs only) is established. Comparison between experimental ARPES and LDA+DMFT+ $\Sigma_{\mathbf{k}}$  data reveals a good semiquantitative agreement. The experimental and theoretical results obtained once again support the AFM scenario of pseudogap formation not only in hole doped HTSC systems [2,3] but also in electron doped ones [4].

### Acknowledgements

This work is partly supported by RFBR Grant 08-02-00021 and was performed within the framework of programs of fundamental research of the Russian Academy of Sciences (RAS) “Quantum physics of condensed matter” (09-II-2-1009) and of the Physics Division of RAS “Strongly correlated electrons in solid states” (09-T-2-1011). IN thanks Grant of President of Russia MK-614.2009.2, interdisciplinary UB-SB RAS project, and Russian Science Support Foundation.

### References

- [1] T. Timusk, B. Statt, Rep. Progr. Phys. 62 (1999) 61; M.V. Sadovskii, Usp. Fiz. Nauk 171 (2001) 539 (Phys. Usp. 44 (2001) 515); M.V. Sadovskii, in: Strings, Branes, Lattices, Networks, Pseudogaps and Dust, Scientific World, Moscow, 2007, p. 357 (in Russian), English version: cond-mat/0408489.
- [2] E.Z. Kuchinskii, I.A. Nekrasov, Z.I. Pchelkina, M.V. Sadovskii, Zh. Eksp. Teor. Fiz. 131 (2007) 908 (J. Exp. Theor. Phys. 104 (2007) 792); I.A. Nekrasov, E.Z. Kuchinskii, Z.V. Pchelkina, M.V. Sadovskii, Physica C 460–462 (2007) 997.
- [3] I.A. Nekrasov, E.E. Kokorina, E.Z. Kuchinskii, M.V. Sadovskii, S. Kasai, A. Sekiyama, S. Suga, JETP 110 (2010) 989. doi:10.1134/S1063776110060099.
- [4] E.E. Kokorina, E.Z. Kuchinskii, I.A. Nekrasov, Z.V. Pchelkina, M.V. Sadovskii, A. Sekiyama, S. Suga, M. Tsunekawa, Zh. Eksp. Teor. Fiz. 134 (2008) 968 (J. Exp. Theor. Phys. 107 (2008) 818); I.A. Nekrasov, et al., J. Phys. Chem. Solids 69 (2008) 3269.
- [5] I.A. Nekrasov, N.S. Pavlov, E.Z. Kuchinskii, M.V. Sadovskii, Z.V. Pchelkina, V.B. Zabolotnyy, J. Geck, B. Buchner, S.V. Borisenko, D.S. Inosov, A.A. Kordyuk, M. Lambacher, A. Erb, Phys. Rev. B 80 (2009) 115124(R).
- [6] A. Georges, G. Kotliar, W. Krauth, M.J. Rozenberg, Rev. Mod. Phys. 68 (1996) 13.
- [7] K. Held, I.A. Nekrasov, G. Keller, V. Eyert, N. Blumer, A.K. McMahan, R.T. Scalettar, Th. Pruschke, V.I. Anisimov, D. Vollhardt, Psi-k Newslett. 56 (2003) 65 (psi-k.dl.ac.uk/newsletters/News\_56/Highlight\_56.pdf); K. Held, Adv. Phys. 56 (2007) 829.
- [8] M.V. Sadovskii, I.A. Nekrasov, E.Z. Kuchinskii, Th. Prushke, V.I. Anisimov, Phys. Rev. B 72 (2005) 155105.
- [9] E.Z. Kuchinskii, I.A. Nekrasov, M.V. Sadovskii, Low Temp. Phys. 32 (2006) 528.
- [10] J. Schmalian, D. Pines, B. Stojkovic, Phys. Rev. B 60 (1999) 667.
- [11] E.Z. Kuchinskii, M.V. Sadovskii, Zh. Eksp. Teor. Fiz. 115 (1999) 1765 (J. Exp. Theor. Phys. 88 (1999) 347).
- [12] A. Damascelli, Z. Hussain, Z.-X. Shen, Rev. Mod. Phys. 75 (2003) 473.

- [13] M. Tsunekawa, A. Sekiyama, S. Kasai, S. Imada, H. Fujiwara, T. Muro, Y. Onose, Y. Tokura, S. Suga, *New J. Phys.* 10 (2008) 073005.
- [14] T. Yoshida, X.J. Zhou, K. Tanaka, W.L. Yang, Z. Hussain, Z.-X. Shen, A. Fujimori, S. Sahrakorpi, M. Lindroos, R.S. Markiewicz, A. Bansil, S. Komiya, Y. Ando, H. Eisaki, T. Kakeshita, S. Uchida, *Phys. Rev. B* 74 (2006) 224510.
- [15] E.Z. Kuchinskii, I.A. Nekrasov, M.V. Sadovskii, *Phys. Rev. B* 75 (2007) 115102.
- [16] O.K. Andersen, *Phys. Rev. B* 12 (1975) 3060;  
O.K. Andersen, O. Jepsen, *Phys. Rev. Lett.* 53 (1984) 2571.
- [17] O.K. Andersen, T. Saha-Dasgupta, *Phys. Rev. B* 62 (2000) R16219;  
O.K. Andersen, et al., *Psi-k Newslett.* 45 (2001) 86;  
O.K. Andersen, T. Saha-Dasgupta, S. Ezhov, *Bull. Mater. Sci.* 26 (2003) 19.
- [18] O. Gunnarsson, O.K. Andersen, O. Jepsen, J. Zaanen, *Phys. Rev. B* 39 (1989) 1708.
- [19] The quasistatic approximation for AFM fluctuations necessarily limits our approach to high-enough temperatures (energies not so close to the Fermi level) (J. Schmalian, D. Pines, B. Stojkovic, *Phys. Rev. B* 60 (1999) 667 and E.Z. Kuchinskii, M.V. Sadovskii, *Zh. Eksp. Teor. Fiz.* 115 (1999) 1765 (*J. Exp. Theor. Phys.* 88 (1999) 347)) so that in fact we are unable to judge e.g. on the nature of low temperature (energy) damping in our model.
- [21] I.A. Zobkalo, et al., *Solid State Commun.* 80 (1991) 921;  
E.M. Motoyama, G. Yu, I.M. Vishik, O.P. Vajk, P.K. Mang, M. Greven, *Nature* 445 (2007) 186.
- [22] M. Hcker, Y.-J. Kim, G.D. Gu, J.M. Tranquada, B.D. Gaulin, J.W. Lynn, *Phys. Rev. B* 71 (2005) 094510.
- [23] K.G. Wilson, *Rev. Mod. Phys.* 47 (1975) 773;  
H.R. Krishna-murthy, J.W. Wilkins, K.G. Wilson, *Phys. Rev. B* 21 (1980) 1003;  
H.R. Krishna-murthy, J.W. Wilkins, K.G. Wilson, *Phys. Rev. B* 21 (1980) 1044.
- [24] R. Bulla, A.C. Hewson, Th. Pruschke, *J. Phys.: Condens. Matter* 10 (1998) 8365.
- [25] N.P. Armitage, F. Ronning, D.H. Lu, C. Kim, A. Damascelli, K.M. Shen, D.L. Feng, H. Eisaki, Z.-X. Shen, P.K. Mang, N. Kaneko, M. Greven, Y. Onose, Y. Taguchi, Y. Tokura, *Phys. Rev. Lett.* 88 (2002) 257001.
- [26] A. Kaminski, H.M. Fretwell, M.R. Norman, M. Randeria, S. Rosenkranz, U. Chatterjee, J.C. Campuzano, J. Mesot, T. Sato, T. Takahashi, T. Terashima, M. Takano, K. Kadowaki, Z.Z. Li, H. Raffy, *Phys. Rev. B* 88 (2002) 257001.